Journal of Power Sources 467 (2020) 228358

Contents lists available at ScienceDirect

Journal of Power Sources

journal homepage: www.elsevier.com/locate/jpowsour

Perspective

Multi-time-scale framework for prognostic health condition of lithium battery using modified Gaussian process regression and nonlinear regression

Xiaoyu Li [a,b], Changgui Yuan [a,b], Zhenpo Wang [a,b,*]

[a] National Engineering Laboratory for Electric Vehicles, School of Mechanical Engineering, Beijing Institute of Technology, Beijing, 100081, China
[b] Collaborative Innovation Center of Electric Vehicles in Beijing, Beijing Institute of Technology, Beijing, 100081, China

HIGHLIGHTS

- Multi-timescale framework is established for forecasting battery SOH and RUL.
- The health features are extracted from partial IC curves from different dimensions.
- A nonlinear regression RUL model is developed by using the GPR-based model.
- Four batteries are used to verify and evaluate the proposed method.

ARTICLE INFO

Keywords:
Lithium-ion batteries
State of health
Incremental capacity analysis
Remaining useful lifetime
Gaussian regression process

ABSTRACT

Prognostic and health management of lithium batteries is a multi-faceted approach that can provide crucial indexes for guaranteeing the reliability and safety of the energy storage system. Herein, a novel multi-time-scale framework is proposed that focuses on short-term battery state of health estimation and long-term remaining useful lifetime prediction. The proposed method extracts four significant features through in-depth analysis of partial incremental capacity and Gaussian process regression with nonlinear regression is applied to forecasting battery health conditions. First, the advanced signal filter methods are employed to smooth initial incremental capacity curves. After that, the significant feature variables are extracted from different degrees such as intercept, slope and peak by linear fitting the partial incremental capacity curves. Second, the significant feature variables feed to Gaussian process regression to establish a short-term battery degradation model using kernel-modified Gaussian process regression. Third, an autoregressive long-term battery prediction model is established by combining the offline short-term battery model with nonlinear regression. The predictive capability, robustness and effectiveness of proposed methods are verified using four datasets with different cycling test conditions and health levels. The results show that the proposed method can give accurate battery health conditions forecasting.

1. Introduction

The excellent performances of lithium-ion batteries such as high energy and power density, low self-discharging and long cycle lifetime have put the rechargeable batteries on an essential position of further energy system [1,2]. Lithium-ion battery has been ubiquitously applied in small-scaled consumer electronics, portable power and large-scale micro-grids, electric vehicles (EVs), airplane, and spacecraft systems [3]. However, the nature of lithium-ion batteries is complex chemistry and nonlinear system and their properties will be decreased with the cycle application such as capacity loss and resistance increased. These changes have potential abilities to trigger system safety issues and reduce reliability [4]. Hence, the advanced prediction and known the status of lithium-ion battery is promising approaches to improve the safety and reliability during the system operation process. The battery health conditions regard as the core parameter in extensive electronic devices and systems, which not only can provide valuable guides for battery maintenance and management but also can give significant references for the system's regular operation and control [5].

Based on the concept of time-scale, the battery health conditions

* Corresponding author. National Engineering Laboratory for Electric Vehicles, School of Mechanical Engineering, Collaborative Innovation Center of Electric Vehicles in Beijing, Beijing Institute of Technology, Beijing, 100081, China.
E-mail addresses: xiaoyu_li187@163.com (X. Li), wangzhenpo@bit.edu.cn (Z. Wang).

https://doi.org/10.1016/j.jpowsour.2020.228358
Received 4 February 2020; Received in revised form 29 April 2020; Accepted 12 May 2020
Available online 1 June 2020

mainly divided into short-term state-of-health (SOH) and long-term remaining useful lifetime (RUL) [6]. Specifically, SOH reflects the degree of current battery health status through the available capacity and RUL refers to the remaining operation time from actual status to the determinate termination criterion [7]. The criterion defines as a proportion of battery rated capacity according to the operational requirement generally set as 70%–80%. There have appeared many comprehensive and representative works for SOH estimation and RUL prediction. The processes of battery SOH and RUL prognostics primarily focus on the external feature parameters such as voltage and current to model battery degradation conditions [8–11]. Reviewing the relevant literature the methods of battery health conditions prognostics can be classified into four different manners: (1) semi-empirical method; (2) model-based method; (3) data-driven method; and (4) feature signal analysis method.

1) *Semi-empirical method:* The approach needs large laboratory test data to analyze the simple correlation between battery capacity fade and stress factors such as temperature and depth-of-discharging (DOD). Based on the battery aging pathways, the method can be concluded as calendar aging and cyclic aging models. The main variables are time, temperature and storage SOC in calendar aging model. Considering battery storage temperature and time, the calendar aging model appears to follow the Arrhenius-like kinetic [12]. Introducing the storage SOC as a stress factor, the Tafel equation fusion in a novel calendar lifetime prediction model is proposed and the calendar semi-empirical model combine with impedance-based electro-thermal model for achieving complete lifetime model [13]. The cycle aging involves complex external environment factors that typically consider the voltage, current, temperature and DOD. Some typical cycle aging models are established by using the cycle number, cumulative charge capacity and current rate [14]. Considering the relationship between lithium loss and Coulombic efficiency, the convex degradation trend of lithium battery is effectively captured and a semi-empirical model is proposed [15]. Under different state-of-charge (SOC) ranges, lithium battery aging mechanisms are fitted using a simple semi-empirical function [16]. These battery degradation models can simplify and easily implement in some specific scenarios. However, battery degradation conditions are influenced by many stress factors. Hence the prognostic accuracy is limited due to the models cannot consider comprehensive and multivariable factors.

2) *Model-based method:* The methods primarily focus on battery degradation mechanism from micro-scaled electrochemistry reaction and macro-scaled physics regulation. According to the different modeling theories, the electrochemistry models can be classified into Pseudo two-dimensional (P2D) model and the Single Particle Model (SPM) [17–19]. Both two-type models can accurately description battery internal and external statuses and characteristics. For battery degradation conditions, the electrochemistry models concentrate on three causes: 1) the loss of lithium ions inventory; 2) the increased solid electrolyte interface (SEI) film; 3) the decreased performance of active electrode materials. These three factors can lead to battery capacity fade and limited maximum available power. Nonetheless, the electrochemistry-based degradation models are usually coupled with many complex partial differential equations (PDEs) that hinder models' practicability and feasibility due to time-consuming and high computational cost [16]. Considering the practical application of battery degradation models, the physics-based models are proposed and the equivalent circuit models (ECMs) attract much attention [20,21]. The models can directly reflect battery degradation according to the relationship between resistance and capacity. The specific parameters of the ECM are identified using different techniques to capture battery degradation and the typical parameter identification methods are some intelligent optimization algorithms, least-square and its extended forms [22–24]. The physics-based models have some merits and they are mainly devoted to constructing an online and closed-loop system. However, the results of battery degradation prognostics are highly dependent on the robustness and reliability of these selected models.

3) *Data-driven method:* These methods take advantage of machine learning algorithms that establish the battery degradation models through training the large of health features (HFs). Support vector machine (SVM), Gaussian process regression (GPR), various neural networks and Monte Carlo are mainly algorithms for battery degradation prognostic. For instance, the HFs are extracted from voltage curves of constant voltage stage during the charging process and the HFs are regarded as input variables for the SVM to build a battery degradation model [25]. Similarly, the HFs are obtained from the voltage evolved curves of constant current stage during the charging process and the GPR algorithm is utilized to model battery degradation using the HFs and available capacity series [26,27]. Based on the correlation between resistances and capacity loss, the extreme learning machine builds the battery degradation model [28]. Sample Entropy combining with relevance vector machine (RVM) as an important tool to capture the underlying correspondence between the discharging voltage and capacity loss [29]. The data-driven methods do not need relevant knowledge background and have excellent nonlinear properties. However, the methods require high-quality training data to ensure the robustness and stability of the training models.

4) *Feature signal analysis method:* The signal analysis methods merge the external battery features with the internal chemistry process and some electrochemical analysis techniques are employed to forecast battery degradation. The incremental capacity analysis (ICA) analyzes the capacity-changed rate under specific voltage intervals during charging/discharging process. IC curves are more sensitive to battery degradation. The peak positions of IC curves and areas of IC curves are the typical features to capture battery degradation [30]. The differential voltage analysis (DVA) can also reflect the status of battery degradation through the interval between two peak points [31,32]. The differential thermal voltammetry (DTV) focuses on the battery surface temperature gradient under corresponding voltage interval during charging/discharging process. The peak positions of DTV curves are applied to quantitatively analyze the battery degradation conditions [33]. Summary, the signal analysis methods can effectively map the battery health conditions with feature parameters of these three specific analysis methods. The methods also combine with some intelligence regression algorithms, which are considered the mainstream approaches in battery degradation forecasting, but there exist some limitations that have to overcome. For instance, these curves easily suffer from noise perturbations and these curves usually need full charging/discharging process.

To overcome these drawbacks, the author proposed a partial IC curves analysis method to estimate battery health conditions in previous publications [3,6,34]. The proposed method can cover the dominating voltage ranges and some features are extracted from IC curves tactfully handle with the noise problem. Additionally, coupled dual GPR-based models are proposed to estimate battery SOH and predict battery RUL on a multi-time-scale. However, there are some limitations need to improve and enhance such as feature extraction and model construction. Motivating by this thought, the targets of this paper are to extract robust features and establish flexible model.

As mentioned above, the main contributions of this study are forecasting short-term battery SOH and long-term RUL with a novel framework through merging data-driven and signal processing methods. In this framework, a state-space model of battery degradation is established using GPR algorithm with the features of partial IC curves and then nonlinear regression is employed to predict battery long-term RUL according to first hit time theory. Specifically, an advanced filter method is proposed to smooth the original IC curves and a linear regression algorithm is applied to fit partial IC curves. Then four feature variables are extracted from intercept, slope and peak of these fitted lines. Secondly, a modified kernel GPR-based algorithm is utilized to establish a flexible state-space model of battery degradation for short-term SOH estimation. Then the relations between cycle number and feature variables are constructed by using nonlinear functions. After that, the feature

variables are updated and fed into the offline GPR-based model. Meanwhile, the battery capacity with the corresponding cycle number is regarded as output results of predicted long-term battery RUL. Finally, the proposed framework of battery health condition forecasting is verified by using four aging datasets from NASA data repository.

2. Battery aging phenomena and incremental capacity analysis

In this section, the characteristics of the aging batteries are extracted through incremental capacity analysis method. Here, the battery the battery aging schedule, two filter methods and the method of feature extraction are presented in detail.

2.1. Battery aging experimental data analysis

The experimental data are obtained from the data repository of NASA Ames Prognostics Center of Excellence [35]. Here, the four tested batteries labeled 5#, 6#, 7#, and 18# comprise of commercially available 18,650-size lithium-ion batteries with length 65 mm and diameter 18 mm, which are produced by Idaho National Laboratory. The cut-off voltages of four batteries are 2.7 V and 4.2 V during normal operation conditions, respectively. The aging cycle test is achieved through three traditional schemes including constant-current and constant-voltage charge (CC-CV) mode, constant current (CC) discharge at room temperature (24 °C). The detailed experimental profiles are summarized in Table 1.

The four batteries are carried out at the same charging regime with CC-CV modes. The evolution profiles of current and voltage are described in Fig. 1(a). In the CC stage, the charging current holds 1.5A until the evolved voltage reaches to the upper cut-off voltage of 4.2 V, and then the CV regime is executed to keep the constant voltage until the charging current drops to 20 mA the charging process completion. After that, the discharging scheme is carried out with continued current 2A until the voltages of the four batteries drop to the preset discharging cut-off voltages 2.7 V, 2.5 V, 2.2 V and 2.5 V for battery 5#, 6#, 7#, and 18#, respectively. The capacities degradation trends of the four batteries are presented in Fig. 1(b). Due to some capacity regeneration phenomena, the capacity degradation curves are not in the smooth trends of monotone decreasing with the aging procedure. This small-range fluctuation of capacity regeneration brings about the nonlinear relationship between battery capacity and the cycle number, which puts forward higher technical requirements for forecasting battery health conditions. Hence, some robust features are necessary to map the battery capacity degradation and to construct a reliable and flexible battery degradation model. The feature extraction and application are descriptions in the next part.

2.2. Incremental capacity curve analysis and filter

Considering the uncontrollable and unpredicted service conditions of these batteries, the charging process can be regarded as an ideal choice for researching this issue of battery degradation. Combining the constant voltage and current phenomena with electrochemistry theory, the IC curves and ICA method are known as an effective and mainstream approach for modeling and estimation battery health conditions. Based on the principle of capacity increment, the battery capacity and voltage should be known beforehand and the two parameters can be calculated as follows,

$$Q = \int_{\tau=1}^{t} I d\tau \tag{1}$$

$$V = f(Q), Q = f^{-1}(V) \tag{2}$$

where t and V are charging time and voltage, respectively. I refers to the constant current during the charging CC stage. According to the Eqs. (1) and (2), the IC curve can be calculated as

$$\left(f^{-1}\right)' = \frac{dQ}{dV} = \frac{I \cdot dt}{dV} = I \cdot \frac{dt}{dV} \tag{3}$$

Due to the original IC curves are vulnerable to the measured noises, some filters are introduced to obtain filter IC curves for the sake of disclosing the intrinsic properties. Here two general filter algorithms named Gaussian filter (GS) and Savitzky-Golay (SG) filter methods are compared to analyze the smooth results. GS method is usually used for the signal process by separating the low-frequency signals from the higher frequency noises of historical data points. The GS method is described as follows,

$$G(x) = \frac{1}{\sigma\sqrt{2\pi}} exp\left(\frac{-(x-\mu)^2}{2\sigma^2}\right) \tag{4}$$

where μ is window size, which is set to a smaller number because $\mu/2$ sample points cannot filter for the head and the tail of the sample series. The parameter σ is called standard deviation that used to determine the smooth degree for the initial IC curve. The main limitation of this method ignores the head and the tail of the sample series.

SG filter belongs to a type of low-pass filter, well-adapted for data smoothing, which has excellent ability in high-frequency digital signal filter along with the noise based on local least-squares polynomial approximation algorithm [36]. The most attractive property is the filter method can maintain the shape and height of waveform peaks, which is quite suitable for filtering the IC curves to ensure high-quality features. The simple construction of the filter is described as follows,

$$y(i) = \sum_{j=-m}^{j=m} \frac{1}{N} C_j x(i+j) \tag{5}$$

where $x(i)$ is the original input signals and $y(\cdot)$ is the resultant output signals, C_j is the coefficient given by the SG filter. N is the number of convoluting integers, which is equal to the smoothing window size ($2m + 1$). Given the space constraints, readers can refer to the relevant publication for more detailed description of the SG filter algorithm. The detailed calculation process of the filter method is listed in Table 2.

Compared with the GS method, the main contribution of the SG filter method is to use a weighted average of its neighbors to smooth each sample point. Typically, the SG filter method can obtain more steady and smooth IC curves, hence the method can retain more critical information. In this study, the parameters of the SG method are selected through a least square algorithm. Fig. 2(b) shows the results of the two methods for smoothing the initial IC curve of the first cycle of the battery 6#. Obviously, the initial IC curve can be smoothed by both the two filter methods. However, SG filter method has excellent performance in

Table 1
The four batteries' specific cycle condition.

Battery label	Batteries' cycle condition				
	Charging cut-off voltage (V)	Discharging cut-off voltage (V)	Charging constant current (A)	Discharging current (A)	Temperature (°C)
5#	4.2	2.7	1.5	2	24
6#	4.2	2.5	1.5	2	24
7#	4.2	2.2	1.5	2	24
18#	4.2	2.5	1.5	2	24

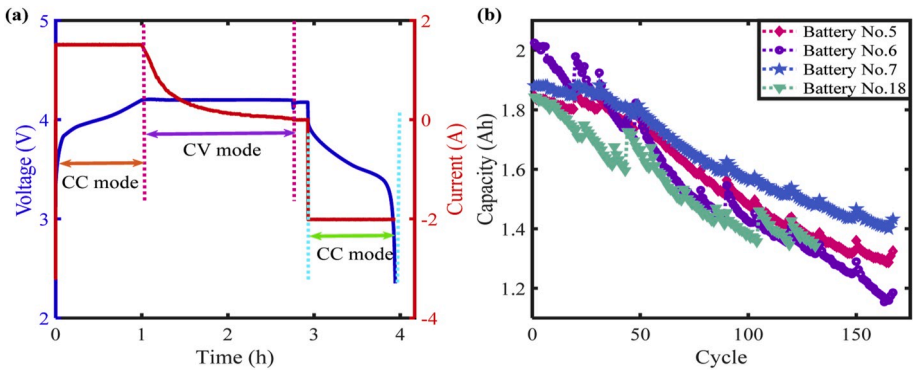

Fig. 1. The battery aging cycle schemes and capacity degradation profiles: (a) A completed aging cycle test for voltage and current; (b) capacity degradation curves of the four batteries.

Table 2
The savitzky-golay filter.

(1) Initialization $N = 2m + 1$ $x = [x_{-m}, x_{-m+1}, \ldots, x_{m-1}, x_m]$
(2) Fit data points by polynomial $y_i = a_0 + a_1 x_i + a_2 x_i^2 + \cdots + a_{k-1} x_i^{k-1}$ $Y_{(2m+1)\times 1} = X_{(2m+1)\times k} \cdot A_{k\times 1} + E_{(2m+1)\times 1}$
(3) Least-squares solution of A $\widehat{A} = (X^T \cdot X)^{-1} \cdot X^T \cdot Y$
(4) The filtering result of Y $\widehat{Y} = X \cdot A = X \cdot (X^T \cdot X)^{-1} \cdot X^T \cdot Y$

capturing the peak points from the IC curve. Meanwhile, the SG method can smooth the head and the tail of the IC curve, as shown in subfigure of Fig. 2(b). Therefore, the SG method is applied to smooth the IC curves.

2.3. Features extraction of battery degradation based on a linear regression algorithm

Battery degradation process contains complex physical/chemical characteristics such as internal resistance and SEI film increasing, which lead to battery charged capacity fade. However, there exist many barriers to capture battery health conditions because these characteristics cannot be directly measured through battery external parameters. Considering the limited measured parameters, the completed and partial IC curves are taken as general methods to reflect battery health conditions. Based on the principles of IC analysis, here four significant features are first proposed from different degrees of partial IC curves such as peak, intercept and slope.

To describe the trends of battery degradation, the IC curves of battery 6# at intervals of 30 cycles are presented in Fig. 3. The completed IC curves cover almost fully charging voltage ranges from 3.4 V to 4.2 V, which are shown in Fig. 3(a). It is evident that the completed IC curves can be divided into two parts based on the voltage regions one part from 3.4 V to 3.8 V and another from 3.8 V to 4.2 V. The IC curves of the first part have gentle slopes, which cannot tell and reflect the characteristics of battery degradation. In the second part, the corresponding IC curves have distinct changes and the voltage range can cover the primary charging process under different battery health levels, which is shown as zoom figure in Fig. 3(a). The zoom figure shows the features of the second part for identifying the battery degradation and these features are extracted with the voltage interval 15 mV.

In this paper, the significant features are obtained from the second part of the IC curves and cover the range of two extreme points with the voltage region from 3.8 V to 4.1 V, as shown in Fig. 3(b). Here the two extreme points are taken as input features for modeling battery degradation at first. For the sake of illustrating the input features, the peak points of different battery health levels are described in Fig. 3(b). Considering the variation tendency of the significant features in Fig. 3 (b), the linear function is applied to fit the significant features based on least square algorithm. In-depth study, intercept-based and slope-based methods are proposed to take as another two important input features for building battery degradation model. From Fig. 3(c), the intercepts of partial IC curves under different health conditions can be clearly presented through sub-figure and the absolute values of the intercepts are gradually reducing with the battery aging. Meanwhile, the slopes of linear functions have noticeable changes and they have the same properties with the absolute values of the intercepts, as shown in Fig. 3 (d). Hence, four input features are extracted from the partial IC curves through two necessary measures extreme points obtaining and linear fitting and the four features with the battery cycle number are plotted in Fig. 3(e) and (f), respectively. The two figures give an intuitive description of the relationship between extracted four features and battery capacity degradation.

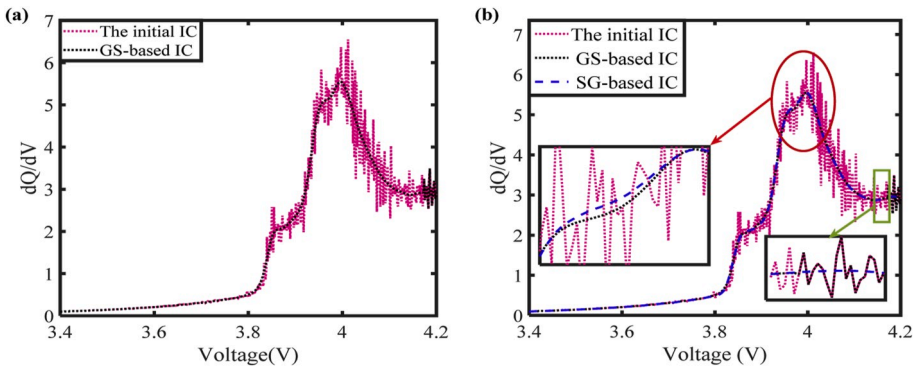

Fig. 2. The IC curve of battery 6#. (a) The initial IC and GS-based curves with measured noise; (b) the comparison of IC curves smoothed by GS-based and SG-based methods.

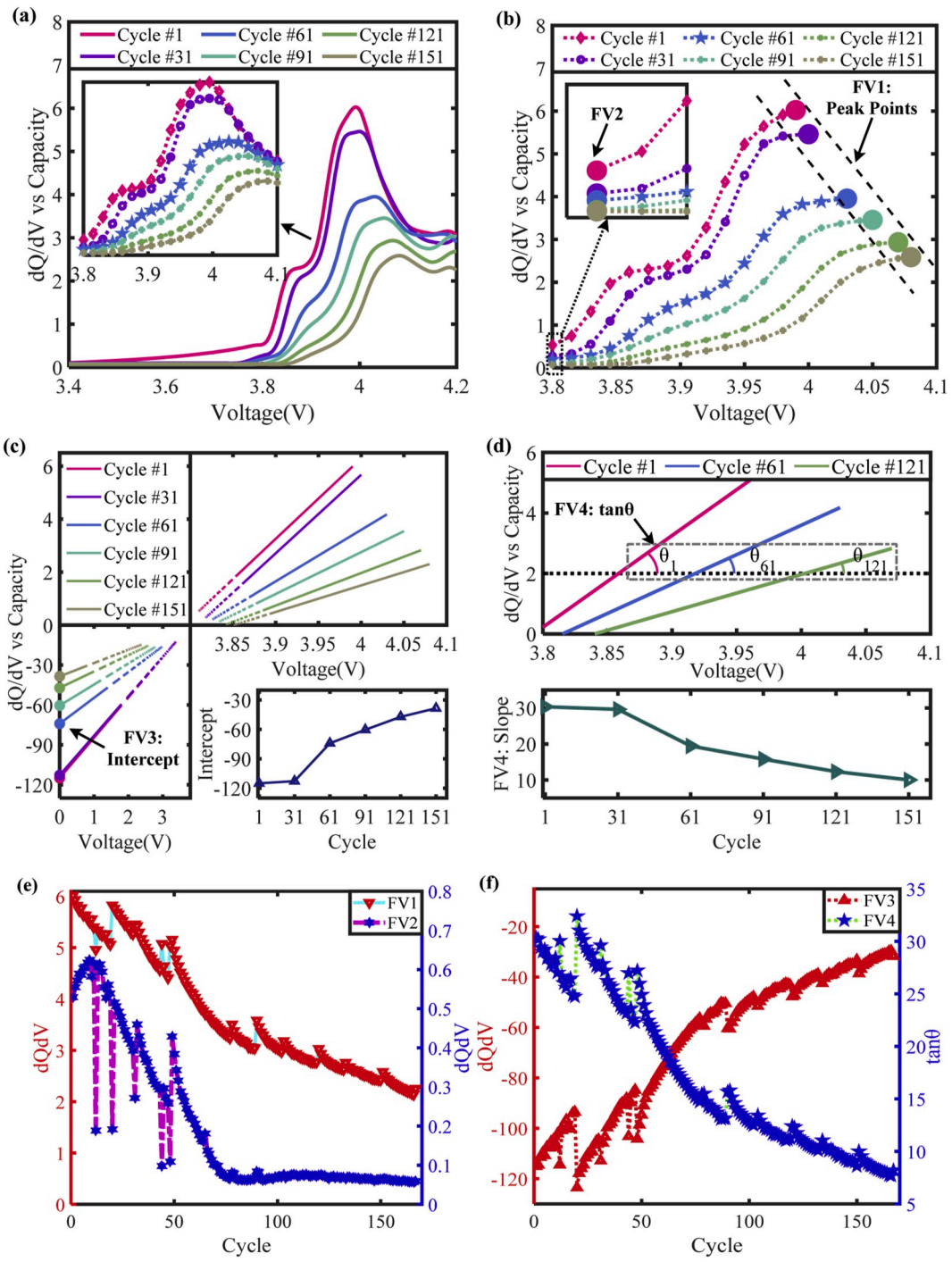

Fig. 3. The IC curves and feature variables of the battery 6# under different cycles. (a) The completed IC curves and the features of partial IC curves under different cycles; (b) two significance features extraction from the partial IC curves; (c) the intercept of the significance evaluation features; (d) the slope of the significance evaluation features; (e) the changes of chosen feature variables (FV1 and 2) with the cycle number; (f) the changes of chosen feature variables (FV3 and 4) with the cycle number.

3. Methodology

With the development of machine learning, GPR is receiving much attention due to the algorithm can provide a principled, practical and probabilistic approach and can give an easy framework for modeling and prediction [37,38]. Compared with other neural network algorithms, which need many decision parameters such as activation function and learning rate, the GPR has concise parameters to build model that more natural to handle and understand the learning process clearly. GPR belongs to non-parameter model and has advantages to solve the high-complexity with low computation cost. Hence, GPR is unutilized to establish high nonlinear battery degradation model for prognostic battery health levels.

3.1. Description of the GPR algorithm

There exist many ways to interpret the GPR algorithm such as function-space and weight-space views. Considering the inference and understand, here the function-space view is used to explain the algorithm. GPR can be regarded as a collection of a limited number of

random variables that follow the Gaussian distribution [39]. GPR is completely determined by mean function $m(\mathbf{x})$ and covariance function $k_f(\mathbf{x}, \mathbf{x}')$, as shown in Eqs. (6) and (7).

$$m(\mathbf{x}) = \mathrm{E}[f(\mathbf{x})] \tag{6}$$

$$k_f(\mathbf{x}, \mathbf{x}') = E\left[(f(\mathbf{x}) - m(\mathbf{x}))(f(\mathbf{x}') - m(\mathbf{x}'))^T\right] \tag{7}$$

where $f(\mathbf{x})$ is the target output and $\mathbf{x}$ is d-dimensional n input vectors, the Gaussian process can be written as

$$f(\mathbf{x}) \sim \mathscr{GP}\left(m(\mathbf{x}), k_f(\mathbf{x}, \mathbf{x}')\right) \tag{8}$$

here is the entire definition of the mean and covariance functions. Typically, for notational simplicity the mean function is set as zero and the covariance function uses the popular squared exponential (SE) kernel that has the specific form as follows,

$$k_f(\mathbf{x}, \mathbf{x}') = \sigma_f^2 \exp\left(-\frac{1}{2}(\mathbf{x} - \mathbf{x}')P^{-1}(\mathbf{x} - \mathbf{x}')\right) \tag{9}$$

where the signal variance $\sigma 2\ f$ refers an output scale amplitude, the diagonal matrix P is the characteristic length scales can be described as $\{l2\ i\}_{1 \le i \le d}$, where d is the number of input vector. In practice, the observation output of model has some noises. Hence, the output of model can be expressed with an implicit function plus Gaussian noises as follows,

$$\mathbf{y} = f(\mathbf{x}) + \varepsilon \tag{10}$$

where $\mathbf{y}$ is the observation output vector $[y_1, y_2, \ldots y_n]$ contains some independent and identically distributed (iid) noises-N(0,σ2 n), which consider from three aspects such as measurement errors, modeling errors, and/or the manufacturing tolerances and so on. Here the prior distribution of observations is denoted as

$$y \sim \mathscr{N}\left(0, K_f(x, x) + \sigma_n^2 I_n\right) \tag{11}$$

$$\begin{cases} \mathbf{K}_f(\mathbf{x}, \mathbf{x}) = \left(k_{ij}\right)_{n \times n} \\ k_{ij} = \sigma_f^2 \exp\left(-\frac{1}{2}(x_i - x_j)^2 P^{-1}\right) \end{cases} \tag{12}$$

in Eq. (11), $\mathbf{K}_f(\mathbf{x}, \mathbf{x})$ is a n-dimensional symmetric positive definite matrix. $\sigma 2\ n\mathbf{I}_n$ relates to the noises and defined as the noise covariance matrix, in which $\mathbf{I}_n$ is a n-dimensional unit matrix. In Eq. (12), the equation k_{ij} can be calculated by the similar degree of the variables x_i and x_j. The value of k_{ij} is increasing with the similar degree of the two variables.

Assume that we have a set of training set $\{\mathbf{x}, \mathbf{y}\}$ in the domain Ω_d. Since GPR is a stochastic process, in which any finite subset of random variables couples with joint Gaussian distributions. Here the test point $\mathbf{x}^*$ and corresponding observation function $\mathbf{y}^*$ together with the joint prior distribution observation Eq. (11) can be denoted as

$$\begin{bmatrix} \mathbf{y} \\ \mathbf{y}^* \end{bmatrix} \sim \mathscr{N}\left(0, \begin{bmatrix} \mathbf{K}_f(\mathbf{x}, \mathbf{x}) + \sigma_n^2 \mathbf{I}_n & \mathbf{K}_f(\mathbf{x}, \mathbf{x}^*) \\ \mathbf{K}_f(\mathbf{x}, \mathbf{x}^*)^T & \mathbf{K}_f(\mathbf{x}^*, \mathbf{x}^*) \end{bmatrix}\right) \tag{13}$$

Adjusting the joint Gaussian prior distribution on $\mathbf{y}$, the posterior distribution of $p(\mathbf{y}^*|\mathbf{x}, \mathbf{y}, \mathbf{x}^*)$ is can be derived as

$$p\left(\mathbf{y}|\mathbf{x}, \mathbf{y}, \mathbf{x}\right) = \mathscr{N}\left(\mathbf{y}^*|\widehat{\mathbf{y}}^*, \sigma^2(\mathbf{y}^*)\right) \tag{14}$$

where the prediction mean $\widehat{\mathbf{y}}^*$ and the prediction covariance $\sigma^2(\mathbf{y}^*)$ are given as follows

$$\widehat{\mathbf{y}}^* = \mathbf{K}_f(\mathbf{x}, \mathbf{x}^*)^T \left[\mathbf{K}_f(\mathbf{x}, \mathbf{x}) + \sigma_n^2 \mathbf{I}_n\right]^{-1} \mathbf{y} \tag{15}$$

$$\sigma^2(\mathbf{y}^*) = \mathbf{K}_f(\mathbf{x}^*, \mathbf{x}^*) - \mathbf{K}_f(\mathbf{x}, \mathbf{x}^*)^T \left[\mathbf{K}_f(\mathbf{x}, \mathbf{x}) + \sigma_n^2 \mathbf{I}_n\right]^{-1} \mathbf{K}_f(\mathbf{x}, \mathbf{x}^*) \tag{16}$$

where $\mathbf{K}_f(\mathbf{x}, \mathbf{x}^*)$ is the covariance between training data and test data. To realize the prediction of model, the hyper-parameters set $\Theta = [\sigma_f, l, \sigma_n]$ need to be solved and optimized by minimizing the negative log marginal likelihood (NLML) as

$$\Theta_{\text{opt}} = \underset{\Theta}{\operatorname{argmin}}\ \text{NLML} \tag{17}$$

where

$$\begin{aligned} \text{NLML} = -\log\ p(\mathbf{y}|\mathbf{x}, \Theta) &= \frac{1}{2}\mathbf{y}^T \left[\mathbf{K}_f(\mathbf{x}, \mathbf{x}) + \sigma_n^2 \mathbf{I}_n\right]^{-1} \mathbf{y} \\ &+ \frac{1}{2}\log\left(\det\left(\mathbf{K}_f(\mathbf{x}, \mathbf{x}) + \sigma_n^2 \mathbf{I}_n\right)\right) + \frac{n}{2}\log 2\pi \end{aligned} \tag{18}$$

Generally, the efficient gradient descent algorithm is used to solve the Eq. (18) by the partial derivatives of the marginal likelihood. The solution procedure as

$$\begin{cases} \dfrac{\partial}{\partial \Theta_i} \log p(\mathbf{y}|\mathbf{x}, \Theta) = \dfrac{1}{2}\left\{\left[\alpha\alpha^T - \left(\mathbf{K}_f(\mathbf{x}, \mathbf{x}) + \sigma_n^2 \mathbf{I}_n\right)^{-1} \dfrac{\partial\left(\mathbf{K}_f(\mathbf{x}, \mathbf{x}) + \sigma_n^2 \mathbf{I}_n\right)}{\partial \Theta_i}\right]\right\} \\ \alpha = \left(\mathbf{K}_f(\mathbf{x}, \mathbf{x}) + \sigma_n^2 \mathbf{I}_n\right)^{-1} \mathbf{y} \end{cases} \tag{19}$$

Once the hyper-parameters are determined, the GPR model is fixed and the test data can be predicted through mean function and covariance function.

3.2. Polynomial regression algorithm

Polynomial regression is a simple regression in statistics, which models the relationship between independent variable x and the dependent variable y using nth degree polynomial. The general polynomial regression can be presented as follows,

$$y = \beta_0 + \beta_1 x + \beta_2 x^2 + \beta_3 x^3 + \cdots + \beta_n x^n + \varepsilon \tag{20}$$

where ε is an unobserved random error with mean zero and β_i refers to the unknown coefficients that are identified offline. Here, the least-squares analysis is applied to compute and infer the coefficients of polynomial regression. In this study, the features of battery degradation are fitted for predicting long-term battery RUL. Next section the GPR-based battery model and nonlinear regression for multi-time-scale battery health conditions are introduced.

3.3. The framework of battery short-term SOH estimation and long-term RUL prediction

Battery health condition prognostics can be divided into short-term SOH estimation and long-term RUL prediction from time-scale, which both play essential roles in energy storage applications. The two parameters can not only ensure the safety and reliability of those storage systems but also can give valuable guidelines for customers and manufacturers. Although the two parameters both reflect battery health conditions, however, they have different principles and theories for battery health prognostics to some extent. Considering the correlation of two parameters, here a coupling method is proposed for joint forecasting battery health conditions. The features of measured external parameters are used to establish the GPR-based battery degradation model for short-term SOH estimation. Then the nonlinear regression is employed to update features to predict the long-term battery RUL.

Specifically, the GPR-based battery degradation model is established by using the features extracted from partial incremental capacity curves for estimating battery SOH and the methods of feature extraction are introduced in section II. The input feature variables such as peaks, intercept and slope, which are collected as $\mathbf{X} = [\mathbf{x}_1, \mathbf{x}_2 \ldots, \mathbf{x}_n]$ where $\mathbf{x}_i$ is a four-dimensional vector and the sequences n is the cycle number of tested battery. The output observation dataset for building the model is a

series of battery available capacities. Once the battery degradation is built, the battery long-term RUL prediction can be carried out through nonlinear regression of the four feature variables. Here combining the GPR-based model with nonlinear regression constructs an auto-regression model for battery short- and long-term health prognostics. After each battery SOH estimation, the degradation features of the battery are continually updated for the off-line GPR-based model until the output capacity reaches to the corresponding cut-off capacity. Then the number of updates is regarded as the battery RUL. It is noticeable that the two models need training in advance before online forecasting battery health conditions.

Two types of general error analysis methods called mean absolute error (MAE) and the root mean square error (RMSE) are applied to make a quantitative analysis of the proposed model for battery health prognostics. The two methods can be denoted as follows,

$$MAE_C = \frac{1}{N}\sum_{i=1}^{N}|y_i - \hat{y}_i^*|, MAE_R = \frac{1}{N}\sum_{i=1}^{N}|L_i - \hat{L}_i^*| \tag{21}$$

$$RMSE_C = \sqrt{\frac{1}{N}\sum_{i=1}^{N}(y_i - \hat{y}_i^*)^2}, RMSE_R = \sqrt{\frac{1}{N}\sum_{i=1}^{N}(L_i - \hat{L}_i^*)^2} \tag{22}$$

where the parameters MAE_C, $RMSE_C$ and MAE_R, $RMSE_R$ are the corresponding values for analysis of the short- and long-term battery health conditions, respectively. The y_i and $\hat{y}_i^*$ are the actual measured values and predicted values for battery SOH, respectively. Similarly, L_i and $\hat{L}_i^*$ are measured and predicted values for battery RUL, respectively. Otherwise, the 95% confidence intervals (CI) of the GPR-based model is employed to assessment of the uncertainty as

$$95\%CI_C = \hat{y}_i^* \pm 1.96 \times \sigma^2(y_i^*) \tag{23}$$

where $95\%CI_C$ is the confidence interval for short-term SOH estimation.

To illustrate the proposed method clearly, here an entire framework of the battery health prognostics based on the GPR model and nonlinear regression is given in Fig. 4. First, the IC curves of batteries are obtained from external measured voltage and current parameters, which are collected from the NASA database. The significant partial IC curves are analyzed and the linear interpolation method is used to fit these curves. From spatial and temporal aspects, the battery cycle number and the corresponding fitted linear are comprehensive consideration. Hence, four features are extracted from different scales of these fitted lines such as peak, intercept and slope. After that, the four features of the partial IC curves are taken as input datasets and are employed to build the GPR-based model for short-term battery SOH estimation. Then the features are undated online to predict battery RUL based GPR model. At last, two error analysis methods are proposed to verify the reliability and accuracy of the proposed model.

4. Battery health prognostics results and discussion

The proposed method of battery health prognostics is verified and analyzed in this section. Here the public battery degradation data of NASA database are employed to analyze the accuracy and stability for the GPR-based battery SOH estimation in qualitative and quantitative. Based on the offline GPR model, the predicted results of battery RUL are online updated and the accuracy of nonlinear regression is verified. Otherwise, the robustness of the coupling battery SOH and RUL prediction model is verified by using the unknown initial health conditions of the four tested batteries.

4.1. Multi-time-scale battery health forecasting based on a proposed model

The proposed GPR-based battery model is utilized to estimate short-term battery SOH by using the four features of different dimensions and the battery RUL is predicted through the nonlinear regression method using continually update feature variables. Here the four tested battery datasets are applied to verify the accuracy and effectiveness of the proposed method. The data of the first 30 cycles are taken as training data for establishing the short-term GPR-based battery model and the residual datasets are applied to test the corresponding model. The results of short-term SOH estimations of the four test batteries (5#, 6#, 7# and

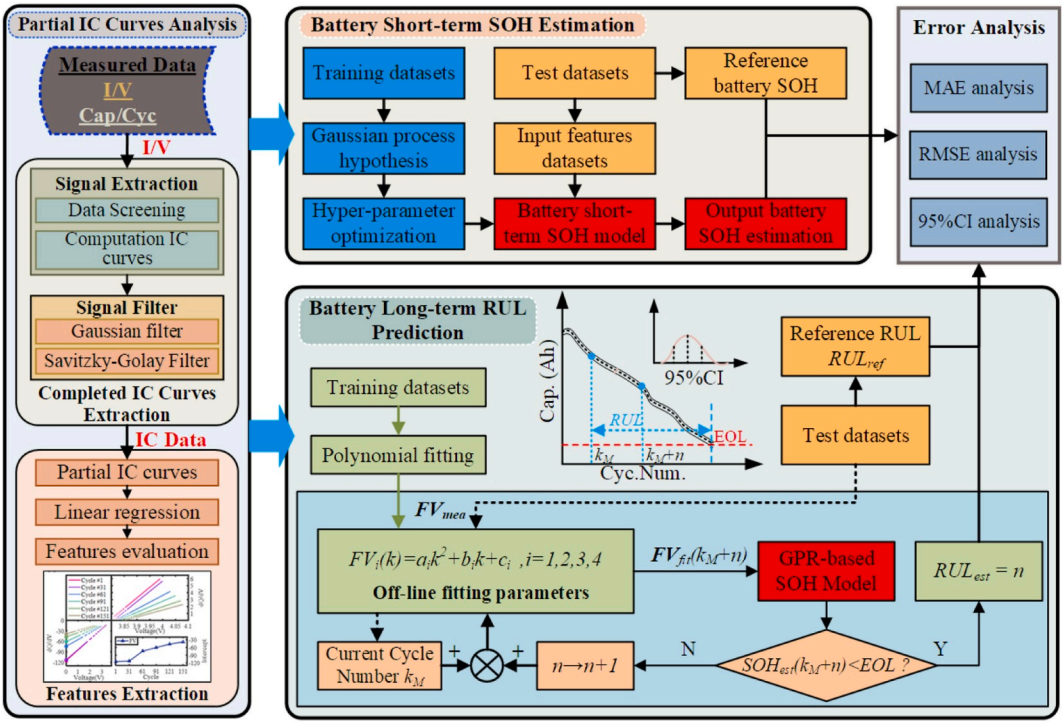

Fig. 4. Flowchart of the dual GPR-based models for short-term and long-term battery health prognostics.

18#) and the relative errors are shown in Fig. 5. The results of battery short-term SOH estimation are presented in Fig. 5(a), (c), (e) and (g). From the four figures, the initial values of battery SOHs are all starting from 1 according to the basic SOH definition. In these figures, the black zones are described the confidence intervals of the models, which are calculated by using Eq. (23) with mean and covariance functions, are employed to present the uncertainty of the models. Generally, the narrower 95% black areas are, the stronger reliability of the estimation models are. From the four figures mentioned above, the zones of the 95% ICs are rather narrow that indicate battery models have excellent reliability. Meanwhile, these models have good accuracy and all relative errors are less than 2%. The results of relative errors of short-term SOH estimation are shown in Fig. 5(b), (d), (f) and (h). Otherwise, the frequencies of each battery relative errors are presented in the subset of the four figures. The majority of frequencies are concentrated on the low error areas and the results also manifest that the proposed GPR-based model has high accuracy.

Due to the battery RUL prediction depends on the offline GPR-based model, the verification and analysis the proposed method of battery long-term RUL prediction should be based on the GPR-based models of the four tested batteries. As illustrated in Fig. 6(a), (c), (e) and (g), the blue lines in each figure are the real RUL values and the prediction RUL values in pink dotted lines. Here the nonlinear regression method is applied to update the input features data for the GPR-based models and the time series of the update are regarded as battery RUL. From the four figures, the initial values of the predicted RUL have bigger relative errors because the nonlinear regression cannot find suitable parameters and the cases can be seen as the coverage process. As shown in Fig. 6(b), (d), (f) and (h), the relative errors and the error frequencies of the RUL prediction for the four batteries are presented. Omitting the initial errors, the maximum errors of the four results are between 10 cycles and 20 cycles. Otherwise, the error frequencies of the four results all concentrate on the ranges from 5 to 25 cycles. Therefore, the battery RUL prediction of the proposed method has satisfactory and robust

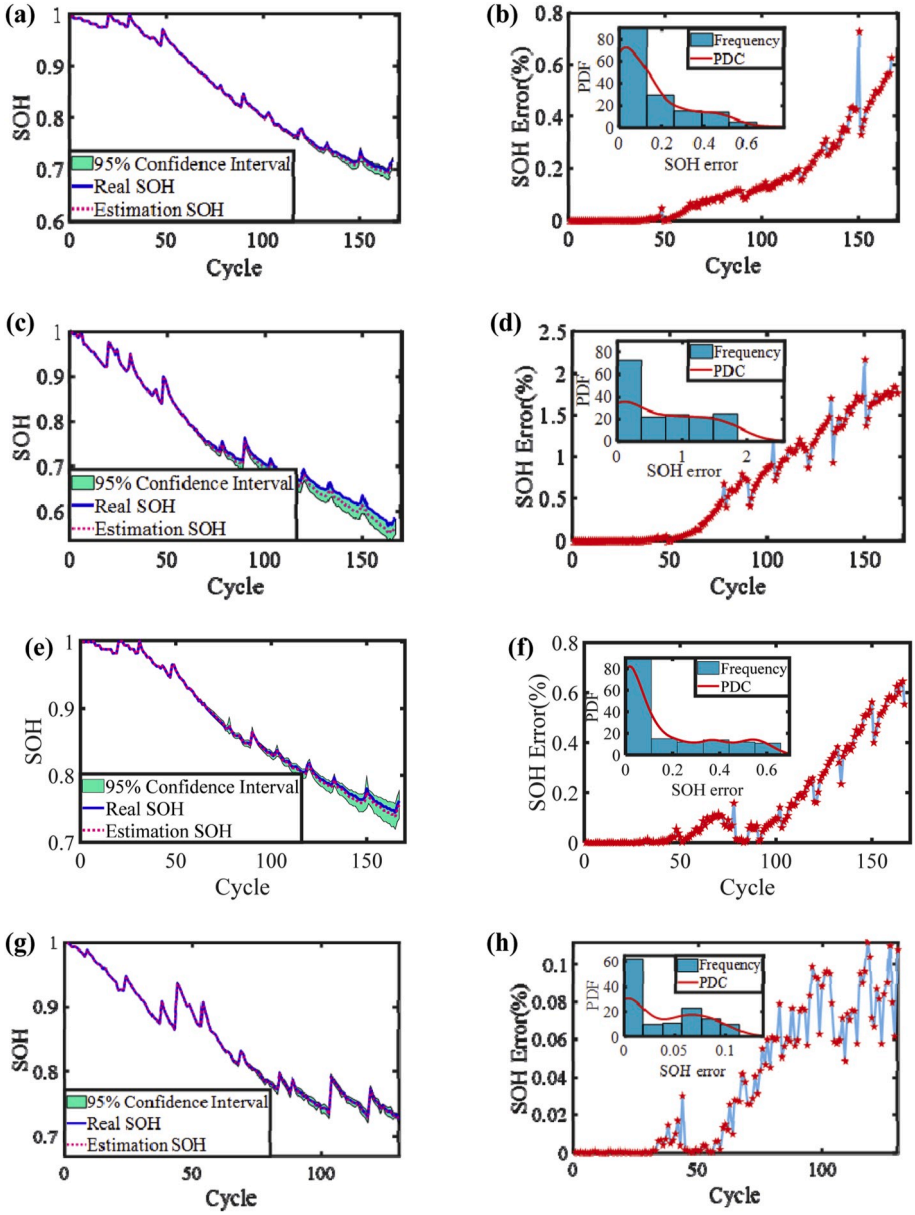

Fig. 5. The short-term battery SOH estimation. (a) Battery short-term SOH estimation for 5#. (b) The relative error of short-term SOH for battery 5#. (c) Battery short-term SOH estimation for 6#. (d) The relative error of short-term SOH for battery 6#. (e) Battery short-term SOH estimation for 7#. (f) The relative error of short-term SOH for battery 7#. (g) Battery short-term SOH estimation for 18#. (h) The relative error of short-term SOH for battery 18#.

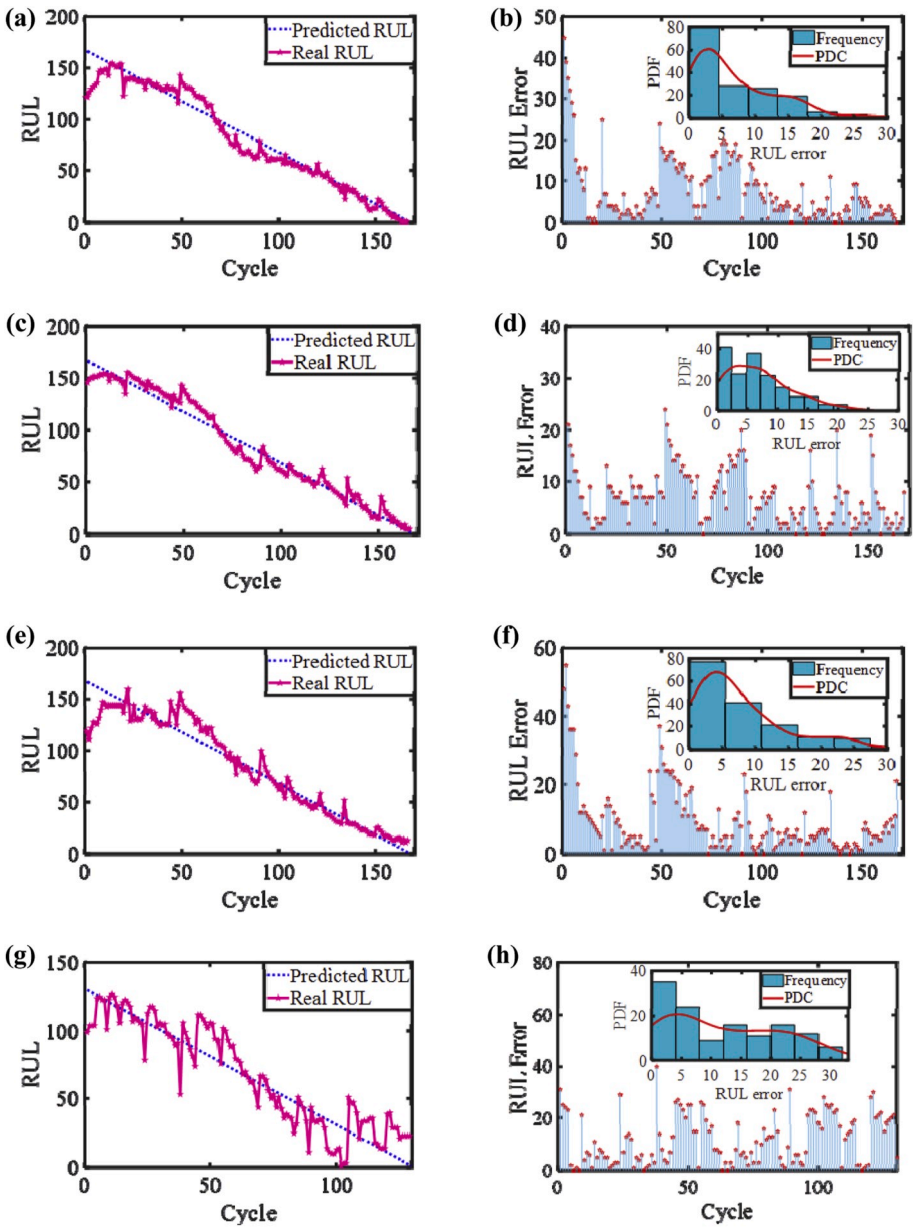

Fig. 6. The long-term battery RUL prediction. (a) Battery long-term RUL prediction for 5#. (b) The relative error of long-term RUL for battery 5#. (c) Battery long-term RUL prediction for 6#. (d) The relative error of long-term RUL for battery 6#. (e) Battery long-term RUL prediction for 7#. (f) The relative error of long-term RUL for battery 7#. (g) Battery long-term RUL prediction for 18#. (h) The relative error of long-term RUL for battery 18#.

performance. The error analysis methods of the MAEs and RMSEs are employed to evaluate the accuracy and effectiveness of the multi-time scale battery health prognostics that are listed in Table 3. The results of *MAEs* and *RMSEs* for the four different batteries are rather small, which also indicates that the proposed method can provide satisfactory and robust prediction performance for battery health conditions.

4.2. Verification the robustness of the proposed model for multi-time scale battery health forecasting

Considering robustness and effectiveness of the proposed method, here a classical verification method is designed by using different starting points of different starting points during whole lifespan for the tested batteries health forecasting. For battery short-term SOH estimation, the feature variables and available capacities are regarded as input and output datasets, respectively. The short-term SOH estimations of the four tested batteries start from the 40th cycle, as shown in Fig. 7(a), (c), (e) and (g). In these figures, the results show the proposed GPR-based model has better robustness and reliability due to the zones of 95% ICs are rather narrow overall process. The relative errors and error frequencies of battery short-term SOH estimations are presented in Fig. 7(b), (d), (f) and (h). All relative errors are almost below 1% and the largest number of error frequencies drop in small range of relative errors. The results manifest that the GPR-based models at different starting points have high robustness and accuracy.

Table 3
Numerical analysis results of dual GPR-based models verification.

Battery label		5#	6#	7#	18#
SOH	MAE_C (Ah)	0.0031	0.0169	0.0007	0.0019
	$RMSE_C$ (Ah)	0.0046	0.0234	0.0011	0.0026
RUL	MAE_R (Cycle)	8.51	6.98	10.40	12.00
	$RMSE_R$ (Cycle)	11.62	8.70	14.12	15.26

The results of offline GPR-based model for RUL prediction from different starting points are shown in Fig. 8(a), (c), (e) and (g). On the contrary, the initial values of the predicted RUL have smaller relative errors in the four figures. Because the nonlinear regression of the corresponding remaining data close to linear that can easily find the suitable parameters and has superior coverage process. Fig. 8(b), (d), (f) and (h) show the relative errors and the error frequencies of the RUL prediction for the four batteries. The maximum errors of the four results are between 5 cycles and 26 cycles. Meanwhile, the error frequencies of the four results primarily concentrate on the ranges from 5 to 25 cycles. Hence, the proposed nonlinear regression method has satisfactory robustness for RUL forecasting under the tested datasets from random starting points. Meanwhile, the MAEs and RMSEs are also employed to analyze the accuracy and effectiveness of the multi-time scale battery health prognostics that are listed in Table 4. The results of error analysis indicate that the proposed method can provide excellent accuracy and robustness for battery health conditions.

5. Conclusion

We present a novel multi-time scale framework of battery health conditions forecasting for estimating short-term SOH and predicting long-term RUL. In this work, we make an intensive study of partial incremental capacity curves. Thereafter, the four training features are extracted from different scales including intercept, slope and peak. The GPR-based model of battery SOH estimation is established by using these features and the RUL prediction has been developed through combining the offline GPR-based model with nonlinear regression. The tested data of four batteries are collected from NASA database under different aging tests, which are applied to verify the accuracy and robustness of the proposed model. The results show that the multi-time scale states of four batteries are accurate, effective, reliable and robust,

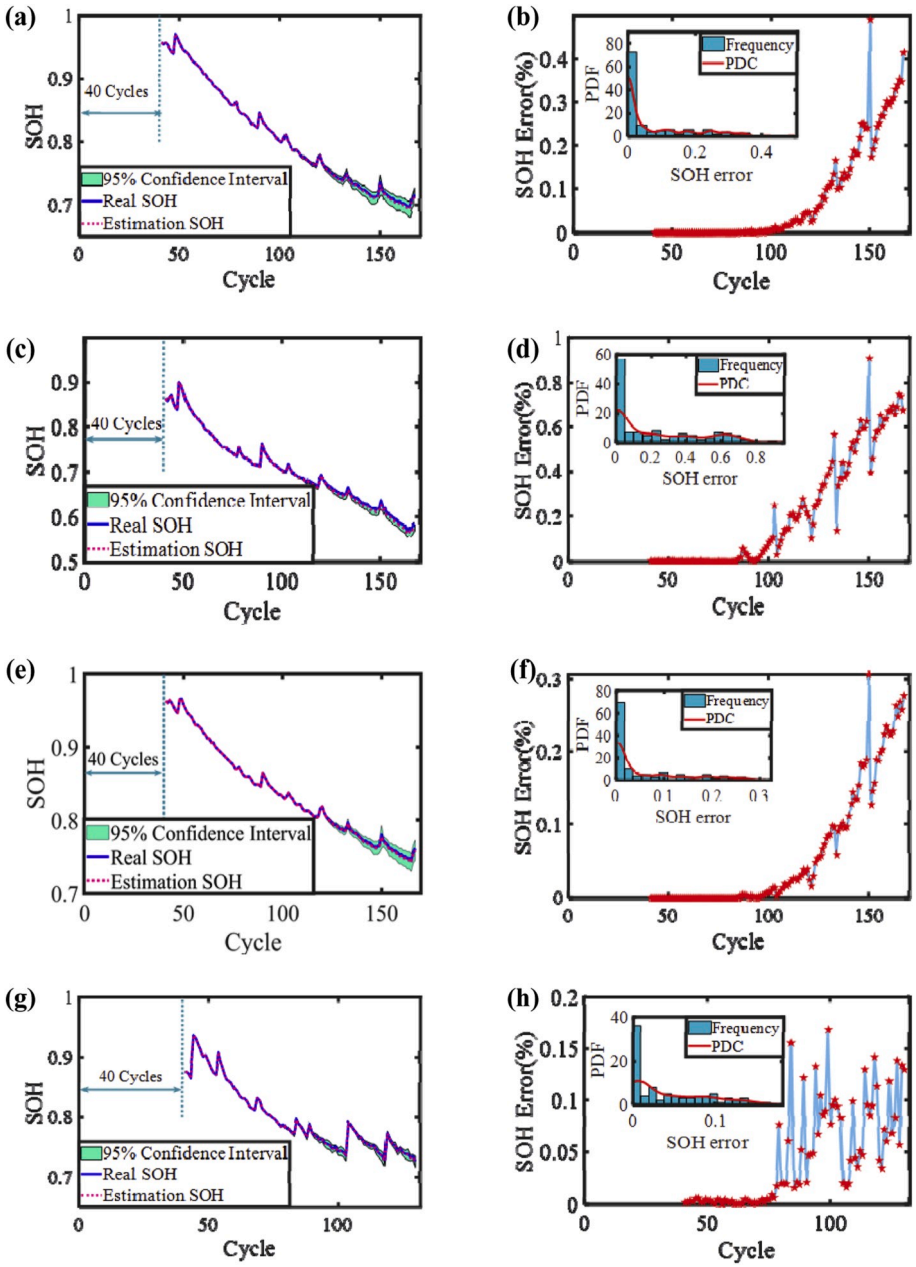

Fig. 7. The short-term battery SOH estimation. (a) Battery short-term SOH estimation for 5#. (b) The relative error of short-term SOH for battery 5#. (c) Battery short-term SOH estimation for 6#. (d) The relative error of short-term SOH for battery 6#. (e) Battery short-term SOH estimation for 7#. (f) The relative error of short-term SOH for battery 7#. (g) Battery short-term SOH estimation for 18#. (h) The relative error of short-term SOH for battery 18#.

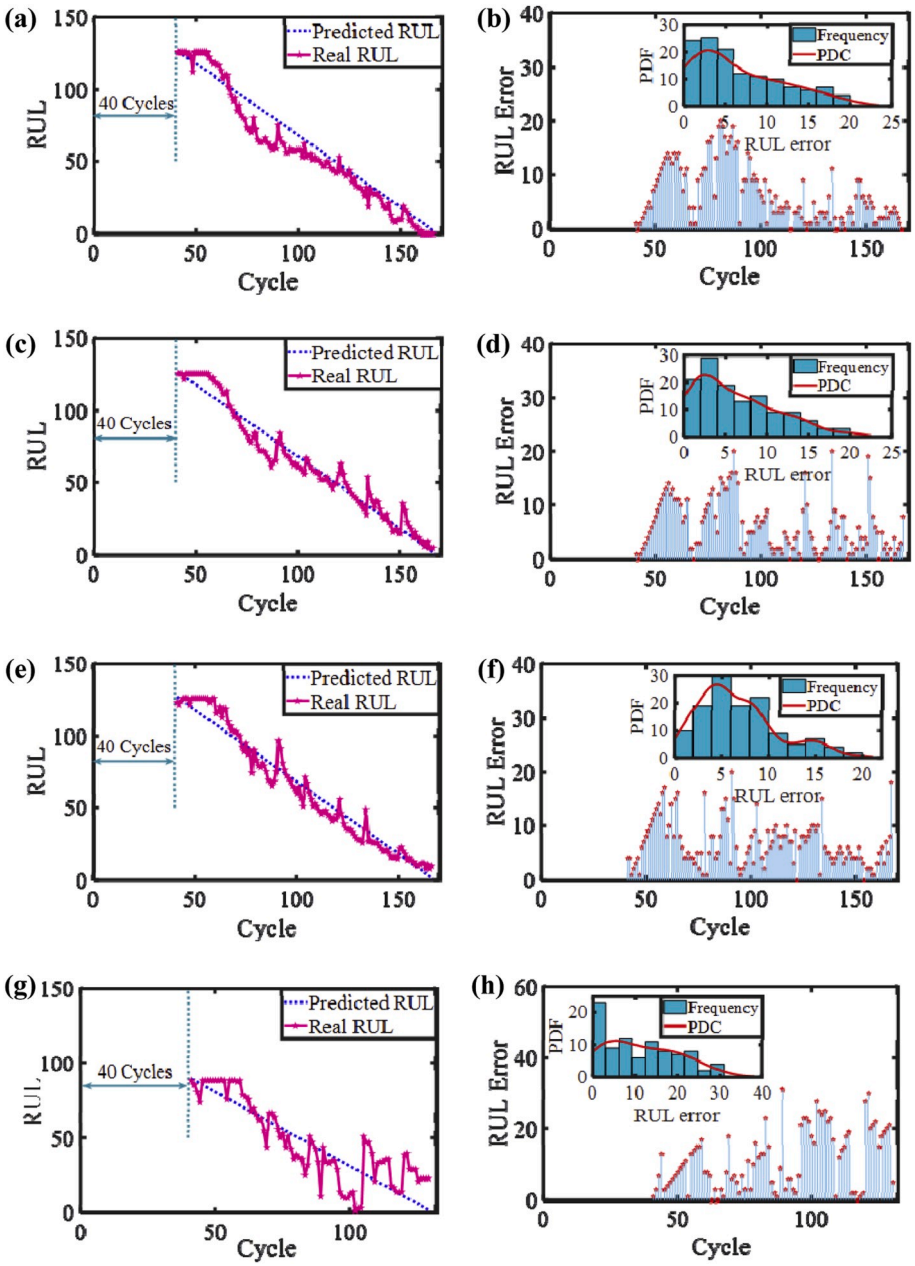

Fig. 8. The long-term battery RUL prediction. (a) Battery long-term RUL prediction for 5#. (b) The relative error of long-term RUL for battery 5#. (c) Battery long-term RUL prediction for 6#. (d) The relative error of long-term RUL for battery 6#. (e) Battery long-term RUL prediction for 7#. (f) The relative error of long-term RUL for battery 7#. (g) Battery long-term RUL prediction for 18#. (h) The relative error of long-term RUL for battery 18#.

Table 4
Numerical analysis results of dual GPR-based models verification.

Battery label		5#	6#	7#	18#
SOH	MAE_C (Ah)	0.0040	0.0073	0.0015	0.0004
	$RMSE_C$ (Ah)	0.0061	0.0101	0.0023	0.0006
RUL	MAE_R (Cycle)	6.44	6.14	6.73	11.46
	$RMSE_R$ (Cycle)	8.32	7.84	7.96	14.16

where the MAEs and RMSEs of the short-term SOH estimation are both less than 2% and the MAEs and RMSEs of the long-term RUL prediction are less than 26 cycles. To future verify the robustness and accuracy of the proposed method, the datasets of random initial health conditions are chosen from for the tested four batteries. The results also show that the proposed method with the significant features exhibits stable, robust performance. The error frequencies of the battery RULs primarily concentrate on the ranges from 5 to 20 cycles. Summary, the proposed method has many advantages such as high accuracy, robustness, and reliability.

Battery degradation has many influence factors, and here we focus on the voltage, current and capacity. However, the temperature effect is also an important factor and cannot be neglected. Thus, the temperature factor will be studied in our next step. Otherwise, the limitations of the proposed method should be suitable for all kinds of batteries and developed a general model in the future.

Declaration of competing interest

The authors declare that they have no known competing financial interests or personal relationships that could have appeared to influence the work reported in this paper.

CRediT authorship contribution statement

Xiaoyu Li: conceived of the presented idea and designed the model and the computational framework. **Changgui Yuan:** assisted with Xiaoyu Li verification the analytical methods. **Zhenpo Wang**: helped supervise the project. All authors discussed the results and contributed to the final manuscript.

Acknowledgments

This work was supported in part by the Scholarship from the China Scholarship Council and in part Graduate Technological Innovation Project of Beijing Institute of Technology.

References

[1] M.S.H. Lipu, M.A. Hannan, A. Hussain, M.H. Saad, A. Ayob, M.N. Uddin, Extreme learning machine model for state-of-charge estimation of lithium-ion battery using gravitational search algorithm, IEEE Trans. Ind. Appl. 55 (4) (2019) 4225–4234.
[2] M. Rana, S.A. Ahad, M. Li, B. Luo, L. Wang, I. Gentle, R. Knibbe, Review on areal capacities and long-term cycling performances of lithium sulfur battery at high sulfur loading, Energy Storage Materials 18 (2019) 289–310.
[3] X. Li, Z. Wang, L. Zhang, C. Zou, D.D. Dorrell, State-of-health estimation for Li-ion batteries by combing the incremental capacity analysis method with grey relational analysis, J. Power Sources 410–411 (2019) 106–114.
[4] Y. Zhu, J. Xie, A. Pei, B. Liu, Y. Wu, D. Lin, J. Li, H. Wang, H. Chen, J. Xu, A. Yang, C.-L. Wu, H. Wang, W. Chen, Y. Cui, Fast lithium growth and short circuit induced by localized-temperature hotspots in lithium batteries, Nat. Commun. 10 (1) (2019) 2067.
[5] R. Xiong, L. Li, J. Tian, Towards a smarter battery management system: a critical review on battery state of health monitoring methods, J. Power Sources 405 (2018) 18–29.
[6] X. Li, Z. Wang, J. Yan, Prognostic health condition for lithium battery using the partial incremental capacity and Gaussian process regression, J. Power Sources 421 (2019) 56–67.
[7] X. Li, L. Zhang, Z. Wang, P. Dong, Remaining useful life prediction for lithium-ion batteries based on a hybrid model combining the long short-term memory and Elman neural networks, Journal of Energy Storage 21 (2019) 510–518.
[8] M. Lucu, E. Martinez-Laserna, I. Gandiaga, H. Camblong, A critical review on self-adaptive Li-ion battery ageing models, J. Power Sources 401 (2018) 85–101.
[9] J. Yang, B. Xia, W. Huang, Y. Fu, C. Mi, Online state-of-health estimation for lithium-ion batteries using constant-voltage charging current analysis, Appl. Energy 212 (2018) 1589–1600.
[10] X. Lai, W. Gao, Y. Zheng, M. Ouyang, J. Li, X. Han, L. Zhou, A comparative study of global optimization methods for parameter identification of different equivalent circuit models for Li-ion batteries, Electrochim. Acta 295 (2019) 1057–1066.
[11] A. Jokar, B. Rajabloo, M. Désilets, M. Lacroix, Review of simplified Pseudo-two-Dimensional models of lithium-ion batteries, J. Power Sources 327 (2016) 44–55.
[12] I. Bloom, B.W. Cole, J.J. Sohn, S.A. Jones, E.G. Polzin, V.S. Battaglia, G. L. Henriksen, C. Motloch, R. Richardson, T. Unkelhaeuser, D. Ingersoll, H.L. Case, An accelerated calendar and cycle life study of Li-ion cells, J. Power Sources 101 (2) (2001) 238–247.
[13] M. Ecker, J.B. Gerschler, J. Vogel, S. Käbitz, F. Hust, P. Dechent, D.U. Sauer, Development of a lifetime prediction model for lithium-ion batteries based on extended accelerated aging test data, J. Power Sources 215 (2012) 248–257.
[14] E. Sarasketa-Zabala, I. Gandiaga, L.M. Rodriguez-Martinez, I. Villarreal, Calendar ageing analysis of a LiFePO4/graphite cell with dynamic model validations: towards realistic lifetime predictions, J. Power Sources 272 (2014) 45–57.
[15] F. Yang, X. Song, G. Dong, K.-L. Tsui, A coulombic efficiency-based model for prognostics and health estimation of lithium-ion batteries, Energy 171 (2019) 1173–1182.
[16] Y. Gao, J. Jiang, C. Zhang, W. Zhang, Y. Jiang, Aging mechanisms under different state-of-charge ranges and the multi-indicators system of state-of-health for lithium-ion battery with Li(NiMnCo)O2 cathode, J. Power Sources 400 (2018) 641–651.
[17] X. Han, M. Ouyang, L. Lu, J. Li, Simplification of physics-based electrochemical model for lithium ion battery on electric vehicle. Part II: pseudo-two-dimensional model simplification and state of charge estimation, J. Power Sources 278 (2015) 814–825.
[18] P. Kemper, S.E. Li, D. Kum, Simplification of pseudo two dimensional battery model using dynamic profile of lithium concentration, J. Power Sources 286 (2015) 510–525.
[19] A.M. Bizeray, J. Kim, S.R. Duncan, D.A. Howey, Identifiability and parameter estimation of the Single particle lithium-ion battery model, IEEE Trans. Contr. Syst. Technol. (2018) 1–16.
[20] X. Hu, H. Yuan, C. Zou, Z. Li, L. Zhang, Co-estimation of state of charge and state of health for lithium-ion batteries based on fractional-order calculus, IEEE Trans. Veh. Technol. 67 (11) (2018) 10319–10329.
[21] Y. Feng, C. Xue, Q. Han, F. Han, J. Du, Robust estimation for state-of-charge and state-of-health of lithium-ion batteries using integral-type terminal sliding-mode observers, IEEE Trans. Ind. Electron. 67 (5) (2019) 4013–4023, 1-1.
[22] Z. Chen, X. Li, J. Shen, W. Yan, R. Xiao, A novel state of charge estimation algorithm for lithium-ion battery packs of electric vehicles, Energies 9 (9) (2016) 710.
[23] X. Li, Z. Wang, L. Zhang, Co-estimation of capacity and state-of-charge for lithium-ion batteries in electric vehicles, Energy 174 (2019) 33–44.
[24] Z. Chen, C.C. Mi, Y. Fu, J. Xu, X. Gong, Online battery state of health estimation based on Genetic Algorithm for electric and hybrid vehicle applications, J. Power Sources 240 (2013) 184–192.
[25] J. Wei, G. Dong, Z. Chen, Remaining useful life prediction and state of health diagnosis for lithium-ion batteries using particle filter and support vector regression, IEEE Trans. Ind. Electron. 65 (7) (2018) 5634–5643.
[26] R.R. Richardson, M.A. Osborne, D.A. Howey, Gaussian process regression for forecasting battery state of health, J. Power Sources 357 (2017) 209–219.
[27] D. Yang, X. Zhang, R. Pan, Y. Wang, Z. Chen, A novel Gaussian process regression model for state-of-health estimation of lithium-ion battery using charging curve, J. Power Sources 384 (2018) 387–395.
[28] H. Pan, Z. Lü, H. Wang, H. Wei, L. Chen, Novel battery state-of-health online estimation method using multiple health indicators and an extreme learning machine, Energy 160 (2018) 466–477.
[29] A. Widodo, M.-C. Shim, W. Caesarendra, B.-S. Yang, Intelligent prognostics for battery health monitoring based on sample entropy, Expert Syst. Appl. 38 (9) (2011) 11763–11769.
[30] X. Tang, C. Zou, K. Yao, G. Chen, B. Liu, Z. He, F. Gao, A fast estimation algorithm for lithium-ion battery state of health, J. Power Sources 396 (2018) 453–458.
[31] L. Zheng, J. Zhu, G. Wang, D.D.-C. Lu, T. He, Differential voltage analysis based state of charge estimation methods for lithium-ion batteries using extended Kalman filter and particle filter, Energy 158 (2018) 1028–1037.
[32] L. Wang, C. Pan, L. Liu, Y. Cheng, X. Zhao, On-board state of health estimation of LiFePO4 battery pack through differential voltage analysis, Appl. Energy 168 (2016) 465–472.
[33] T. Shibagaki, Y. Merla, G.J. Offer, Tracking degradation in lithium iron phosphate batteries using differential thermal voltammetry, J. Power Sources 374 (2018) 188–195.
[34] X. Li, C. Yuan, X. Li, Z. Wang, State of health estimation for Li-Ion battery using incremental capacity analysis and Gaussian process regression, Energy 190 (2020) 116467.
[35] K. Goebel, B. Saha, A. Saxena, J.R. Celaya, J.P. J.I.i. Christophersen, m. magazine, Prognostics in Battery Health Management, vol. 11, 2008, 4.
[36] W.S. Cleveland, E. Grosse, W.M. Shyu, Local regression models, in: Statistical Models in S, Routledge, 2017.
[37] C.E. Rasmussen, Gaussian processes in machine learning, in: Advanced Lectures on Machine Learning, Springer, 2004.
[38] G.O. Sahinoglu, M. Pajovic, Z. Sahinoglu, Y. Wang, P.V. Orlik, T. Wada, Battery state-of-charge estimation based on regular/recurrent Gaussian process regression, IEEE Trans. Ind. Electron. 65 (5) (2018) 4311–4321.
[39] J. Yu, Online quality prediction of nonlinear and non-Gaussian chemical processes with shifting dynamics using finite mixture model based Gaussian process regression approach, Chem. Eng. Sci. 82 (2012) 22–30.